 DOI: 10.1002/eji.202149469 Eur. J. Immunol. 2022. 52: 328–337

Basic

European Journal of Immunology

Immunity to infection

Research Article

A multifunctional mouse model to study the role of Samd3

Annika E. Peters, Konrad Knöpper, Anika Grafen and Wolfgang Kastenmüller

Würzburg Institute of Systems Immunology, Max Planck Research Group at the Julius-Maximilians-Universität Würzburg, Wurzburg, Germany

The capacity to develop immunological memory is a hallmark of the adaptive immune system. To investigate the role of *Samd3 for cellular immune responses and memory development*, we generated a conditional knock-out mouse including a fluorescent reporter and a huDTR cassette for conditional depletion of Samd3-expressing cells. *Samd3* expression was observed in NK cells and CD8 T cells, which are known for their specific function against intracellular pathogens like viruses. After acute viral infections, *Samd3* expression was enriched within memory precursor cells and the frequency of *Samd3*-expressing cells increased during the progression into the memory phase. Similarly, during chronic viral infections, *Samd3* expression was predominantly detected within precursors of exhausted CD8 T cells that are critical for viral control. At the functional level however, *Samd3*-deficient CD8 T cells were not compromised in the context of acute infection with *Vaccinia* virus or chronic infection with Lymphocytic choriomeningitis virus. Taken together, we describe a novel multifunctional mouse model to study the role of *Samd3* and *Samd3*-expressing cells. We found that *Samd3* is specifically expressed in NK cells, memory CD8 T cells, and precursor exhausted T cells during viral infections, while the molecular function of this enigmatic gene remains further unresolved.

Keywords: CD8 T cell · mouse model · NK cell · SAMD3 · viral infection

Additional supporting information may be found online in the Supporting Information section at the end of the article.

Introduction

The ability to form long-lived memory cells is a key feature of the adaptive immune system that provides the basis for protective immunity against recurrent infections. Upon interaction with antigen-bearing DCs, cognate naïve CD8 T cells get activated, proliferate, and differentiate into a spectrum of cellular states [1]. These states range from long-lived, less differentiated memory precursor cells to terminally differentiated, typically short-lived effector cells. A fraction of these precursor cells survive long term and eventually form a stable memory T-cell population. In comparison to their naïve counterparts, memory CD8 T cells express different adhesion molecules and chemokine receptors and have a faster effector response due to preformed mRNAs for IFN-γ or inflammatory chemokines like CCL5 [2]. Although both naïve and central memory CD8 T cells circulate through secondary lymphoid organs, they occupy different niches within these organs. While naïve CD8 T cells are found in the paracortex of the lymph node,

Correspondence: Dr. Annika E. Peters and Prof. Wolfgang Kastenmüller
e-mail: Annika.Peters@med.uni-muenchen.de;
wolfgang.kastenmueller@uni-wuerzburg.de

Correction added on 18 November 2021, after first online publication: The legal statement was changed.

central memory CD8 T cells localize to the interfollicular zones, cortical ridge, and periphery of the paracortex [3]. This strategic positioning at the lymph node periphery allows for a more rapid response against pathogens that drain via the lymph [4]. The strategic positioning of memory T cells at the anticipated site of infection is prominently realized in peripheral tissues. Within epithelial layers, tissue-resident memory T cells (Trm) permanently reside at the previous site of infection and provide superior protection against recurrent infection like with HSV [5]. The functional adaptation to specific cellular microenvironments and tissues, adjusted metabolism, altered homeostasis, and migration patterns as well as enhanced response rates and specialized effector functions are thus hallmarks of memory T cells that require the expression of specific proteins [6]. Indeed, many of these critical proteins have been discovered and encompass transcription factors [7], adhesion molecules, chemokine receptors, enzymes, and membrane transport molecules [8]. Mining publicly available RNA-sequencing data of memory CD8 T cells, *Samd3* (sterile alpha motif domain-containing protein 3) surfaced as a promising candidate due to its temporal expression pattern. Importantly, in the literature the poorly studied protein SAMD3 is often confused with SMAD3 (mothers against decapentaplegic homolog 3)—the well-studied intracellular signal transducer and transcriptional modulator activated by TGF-β [9]. The SAMD protein family is involved in a diverse set of cell biological functions ranging from protein–protein interactions to translational regulation and cell cycle control. Besides protein–protein interactions, SAMD family members also have the ability bind to RNA and lipids thereby reflecting a broad spectrum of potential SAMD3 functions contributing to memory CD8 T-cell differentiation [10, 11]. Besides CD8 T cells, our in silico analysis also indicated a high expression level of *Samd3* in NK cells. This cell type is specialized in killing altered, stressed, and virally infected cells as part of the innate immune system [12, 13]. As CD8 T cells and NK cells can detect altered, stressed, and virally infected cells, we reasoned that SAMD3 might play a key role in immune cells that have the capacity to eliminate such cells. Specifically, we hypothesized that SAMD3 might be essential in regulating the function and/or the differentiation of cytotoxic lymphocytes. Therefore, we decided to test SAMD3 in the context of viral infections to elucidate the, to date, unknown function and exact cellular expression pattern of *Samd3*. In order to investigate the role of this poorly studied molecule, we generated a new mouse model that would allow us to track and conditionally deplete SAMD3 expressing cells as well as to conditionally delete the *Samd3* gene for loss-of-function experiments.

Results

A novel mouse model to study SAMD3

In order to discover new molecules that play an important function in memory CD8 T cells, we interrogated published RNAseq data sets (Immgen.org) comparing naïve versus memory CD8 T cells. This analysis confirmed well-known molecules that are important for memory T-cell development and function including transcription factors (*Eomes, Tbx21, Id2*, and *Bhlhe40*) and chemokine receptors (*Ccr2, Ccr5*, and *Cxcr3*) (Supporting Information Fig. S1). Additionally, we noted several molecules that have not been studied in the context of memory CD8 T cells so far or whose function is unknown like *Samd3*. In order to study the function of SAMD3 and the cellular subsets that express this protein in the context of viral infections, we decided to develop a new mouse model. In particular, we aimed at generating a model that would allow us to address three questions: (i) What is the function of SAMD3? (ii) Which cells express SAMD3? (iii) What is the role of SAMD3 expressing cells? Therefore, we floxed exon2 of the *Samd3* gene using two different lox sequences (loxp and lox2272) and inserted a tdTomato reporter and a huDTR cassette in reverse orientation in the intron between exon2 and exon3 (Fig. 1a). Upon Cre-mediated recombination, exon 2 is removed leading to gene deficiency, while tdTomato and huDTR cassettes are flipped into a forward orientation, allowing the expression of these genes. Thereby, this multifunctional mouse model allows for conditional gene deletion, fluorescent reporting, and DTx-mediated depletion of *Samd3*-expressing cells. Southern blot confirmed site-specific targeting of the Samd3 locus (Supporting Information Fig. S2a). Crossing Ub-Cre x $Samd3^{fl/fl}$ mice resulted in the expected germline recombination of the locus as confirmed by PCR (Supporting Information Fig. S2b and c). For simplification, we termed the resulting mouse line $Samd3^{TD/TD}$ (td*T*omato/hu*D*TR), which was used in this study.

Cellular expression pattern of SAMD3

Having validated our mouse model on a genetic level, we next addressed whether we could identify *Samd3* expressing cells by their tdTomato expression using FACS. In heterozygous $Samd3^{TD/wt}$ mice, we detected dim tdTomato fluorescence in about 2% of all splenocytes (Fig. 1b). In homozygous $Samd3^{TD/TD}$ animals, about 4% of splenocytes were tdTomato positive and expressed on average twice as much tdTomato on a per cell level as indicated by their mean fluorescence intensity (MFI) (Fig. 1b). Interestingly, we observed a significant variance of the tdTomato MFI among littermates, in both $Samd3^{TD/wt}$ and $Samd3^{TD/TD}$ animals (Fig. 1b). Next, we wished to address which cellular subsets express SAMD3. Based on the Immgen database (Immgen.org), we anticipated *Samd3* expression in NK cells, invariant T cells, and CD8 T cells. Indeed, when gating on tdTomato positive cells of $Samd3^{TD/TD}$ mice, the majority (about 65%) were NK cells as indicated by NK1.1 staining and absence of CD3 staining (Fig. 1c). Among T cells, the largest fraction was CD8 positive (about 70%), followed by CD4/CD8 negative invariant T cells and a minor population of CD4 positive T cells (Fig. 1c). NK cells can be further subdivided into four developmental stages based on CD27 and CD11b expression with CD11b single positive cells being most and double negative cells being least differentiated [14]. Among double negative NK cells, only about 20% were

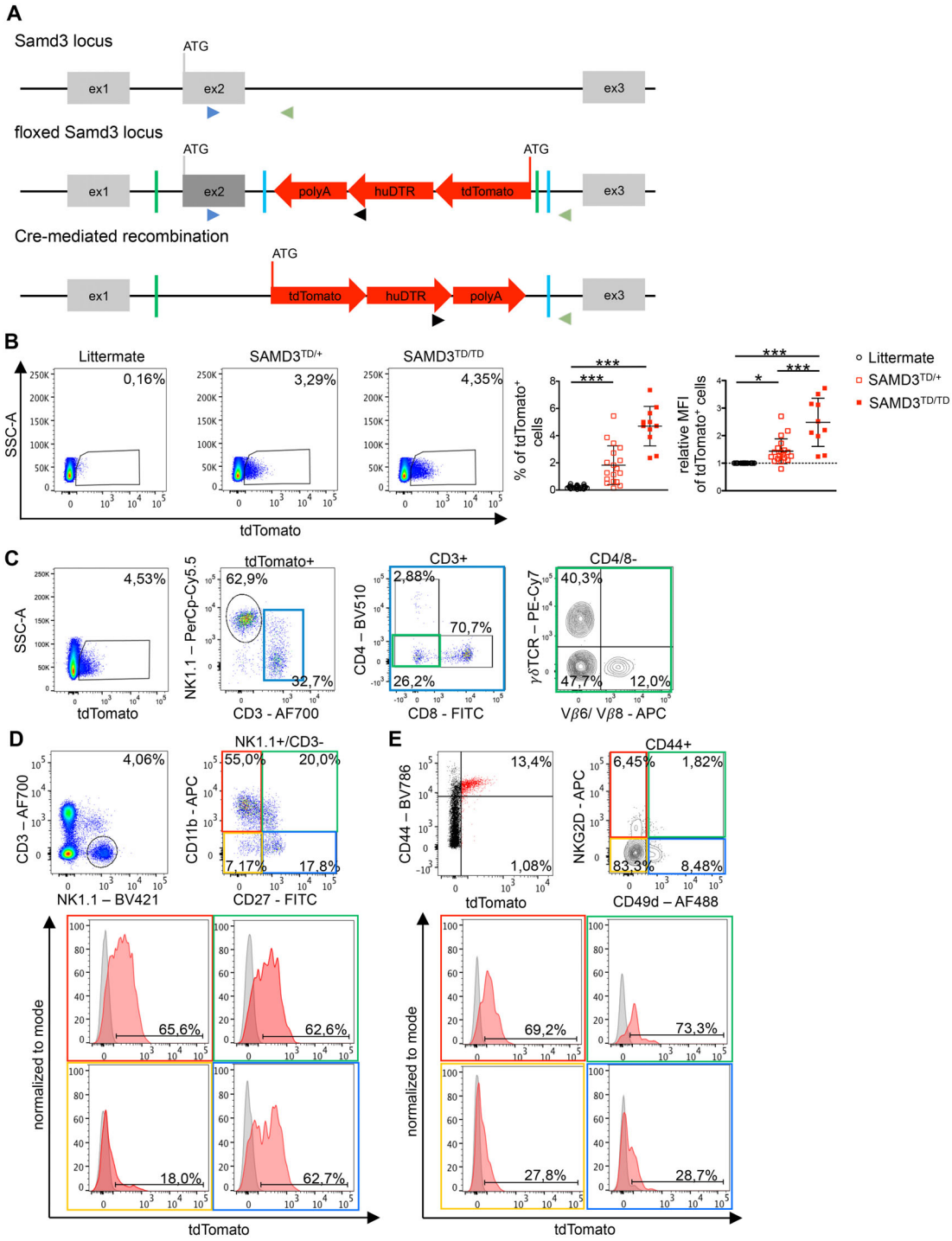

Figure 1. NK cells and CD8 T cells are the major cell types expressing the *Samd3*-reporter tdTomato. (A) Depiction of the modification of the *Samd3* locus. The upper panel shows the wild-type *Samd3* locus. The middle panel shows the floxed Samd3 locus. The exon 2 of the locus and a reverse orientated tdTomato-huDTR-cassette is flanked by loxP sites. Upon Cre mediated recombination (lower panel), the exon 2 is floxed out and the tdTomato-huDTR-cassette is flipped into direct strand orientation onto the ATG of the exon 2. Ex = exon; polyA = poly adenylation motif inducing transcriptional stop; loxP, lox2272 = different lox sites, each recognized by Cre recombinase shown as green and blue lines, respectively. The arrow heads indicate the genotyping primers used. Blue arrowhead: primer_01F, green arrowhead: primer_02R; black arrowhead: primer_04R. (B-F) Flow cytometry analysis of splenocytes comparing Samd3$^{TD/+}$, Samd3$^{TD/TD}$, and littermate control mice. (B) Representative flow cytometry analysis and statistical quantification of the frequency and the MFI of tdTomato expressing cells. (C-E) Representative flow cytometry plots of Samd3$^{TD/TD}$ mice for tdTomato expressing cells classified by expression of (C) lineage-specific markers (NK1.1, CD3, CD4, CD8, γδ TCR, Vβ6/Vβ8), (D) NK cells subsets based on CD11b and CD27 expression, and (E) CD44+ CD8 T cell subsets based on NKG2D and CD49d expression. Parental gating is indicated above the flow cytometry plots. All data are representative of at least two independent experiments ($n \geq 3$ mice per experiment). Error bars indicate SD, and statistical analysis was done with one-way ANOVA using GraphPad. *p-value < 0.05; **p-value < 0.01; ***p-value < 0.001.

tdTomato positive (Fig. 1d). By contrast, among all other NK cell subsets more than 60% were expressing tdTomato. Also, in CD8 T cells, SAMD3 expression was restricted to CD44hi/memory CD8 T cells (Fig. 1e). In particular, antigen-induced NKG2D+ memory CD8 T cells [15] showed a high frequency of tdTomato positive cells (about 70%). So-called virtual memory T cells that are identified by CD49d expression [16] as well as double negative (CD49-/NKG2D-) memory CD8 T cells encompassed only minor fractions of tdTomato positive cells. In summary, Samd3 $^{TD/TD}$ mice as well as Samd3$^{TD/WT}$ mice (Supporting Information Fig. S3) showed tdTomato expression primarily in differentiated NK cells and memory phenotype CD8 T cells in noninfected animals.

The huDTR cassette allows efficient depletion of SAMD3 expressing cells

Next, we wanted to test whether the huDTR cassette is functionally expressed in *Samd3* $^{TD/WT}$ mice enabling us to conditionally deplete SAMD3 expressing cells. Specifically, we treated *Samd3* $^{TD/WT}$ mice with diphteria toxin (DTx) for three consecutive days and analyzed the spleen 4 days later (Fig. 2a). At this point in time, tdTomato-positive cells had been fully depleted underscoring the efficiency of this model (Fig. 2b). Four days after depletion, the total NK cell numbers were reduced by about 50% as compared to nondepleted animals, in line with about 60% of all NK cells expressing td*T*omato/hu*D*TR (TD) (Fig. 2c). When further studying the composition of the remaining NK cells, we noted a shift toward CD11b/CD27 double positive NK cells and a relative loss of fully differentiated CD11b single positive NK cells after DTx treatment (Fig. 2d). Based on the developmental trajectory and the similar, relative SAMD3 (TD) expression between CD27 or CD11b expressing NK cells we conclude that the observed shift is based on a compensatory mechanism by SAMD3 negative cells that newly develop in the bone marrow rather than unequal depletion efficiency among subsets. Besides NK cells, the DTx-mediated depletion of SAMD3 expressing CD8 T cells was also highly efficient and led to a significant relative loss of CD44+ memory T cells in uninfected mice (Fig. 2e). In conclusion, we only detected minor alterations with regard to the fraction of memory CD8 T cells that expressed CD49d or NKG2D following depletion of Samd3 expressing cells (Fig. 2f). Having fully validated our trifunctional mouse model to interrogate SAMD3 and SAMD3-expressing cells, we next applied this mouse model to study SAMD3 in the context of infections.

SAMD3 is expressed in antiviral memory CD8 T cells

In order to investigate whether SAMD3 plays a functional role in CD8 T cells, we infected gene-deficient *Samd3*$^{TD/TD}$ mice or littermate controls with VV-OVA i.p. and analyzed the spleen on d8, d30, and d60 (Fig. 3a). Using multimer staining to identify CD8 T cells that were specific for the immunodominant viral epitope B8R, we found similar relative and absolute numbers when comparing *Samd3*$^{TD/TD}$ and littermate controls over time (Fig. 3b). Also, when analyzing CD8 T cell subsets using standard surface markers KLRG1 and CD127 to identify effector cells and memory precursor cells, respectively, we detected no significant differences between *Samd3*$^{TD/TD}$ and littermate controls (Fig. 3c and Supporting Information Fig. S4a). Recently, another important memory CD8 T-cell subset marked by CX_3CR1 expression has been established [17, 18]. CD8 T cells with a high expression level of this chemokine receptor have a very high cytotoxic capacity, while CD8 T cells with an intermediate level have a high proliferative potential. However, among antigen-specific CD8 T cells, we found a similar expression of CX_3CR1 between Samd3$^{TD/TD}$ and littermate controls throughout the analyzed points in time (Supporting Information Fig. S4b). These data argue that SAMD3 is not involved in the differentiation or survival of memory CD8 T cells. On a functional level, we further observed that *Samd3*-deficient mice had normal capacity to produce the inflammatory cytokines IFN-γ, TNF-α, and IL2 upon antigen-specific restimulation ex vivo (Fig. 3d and data not shown). So far, we compared antigen-specific CD8 T cells between WT and *Samd3*-deficient animals after acute viral infection and did not observe significant differences with regard to differentiation or function. Next, we aimed to address which fraction of antigen-specific CD8 T cells expressed SAMD3 (tdTomato) over time. In homozygous *Samd3*$^{TD/TD}$ mice, we observed that the fraction of tdTomato-positive cells increased from about 10% on d8 to about 40% on d60 postinfection (Fig. 3e). Interestingly, the total numbers of tdTomato expressing B8R-specific CD8 T cells and their MFI for tdTomato remained unaltered over time. By contrast, tdTomato-negative B8R-specific CD8 T cells contracted by about 90% during the transition to memory (Fig. 3e). This finding raised the possibility that SAMD3 expression on d8 postinfection identifies antigen-specific CD8 T cells with a high memory potential that survive long term. Consistently, SAMD3-expressing cells were enriched among CD8 T cells that expressed CD127 positive or CX_3CR1 at intermediated levels, while they were less frequent among KLRG1 expressing terminally differentiated CD8 T cells (Fig. 3f and Supporting Information S4c/d). To further investigate this notion, we interrogated published scRNAseq data on antigen-specific CD8 T cells at different points in time following LCMV infection [19, 20]. *Samd3* expression was detectable in activated CD8 T cells as early as d6 postinfection and in line with our previous data increased over time (Fig. 3g). However, *Samd3* expressing cells did not comprise a unique subset among memory T cells or their precursors (Supporting Information Fig. S5a–c).

SAMD3 is not required for the recall capacity of memory CD8 T cells

Having established that SAMD3-expressing cells are specifically enriched within the memory CD8 T-cell population and its precursors, we next focused on a potential role of SAMD3 in memory CD8 T cells. To test this idea, we infected gene-deficient *Samd3*$^{TD/TD}$ mice and littermate controls with VV-OVA i.p. and

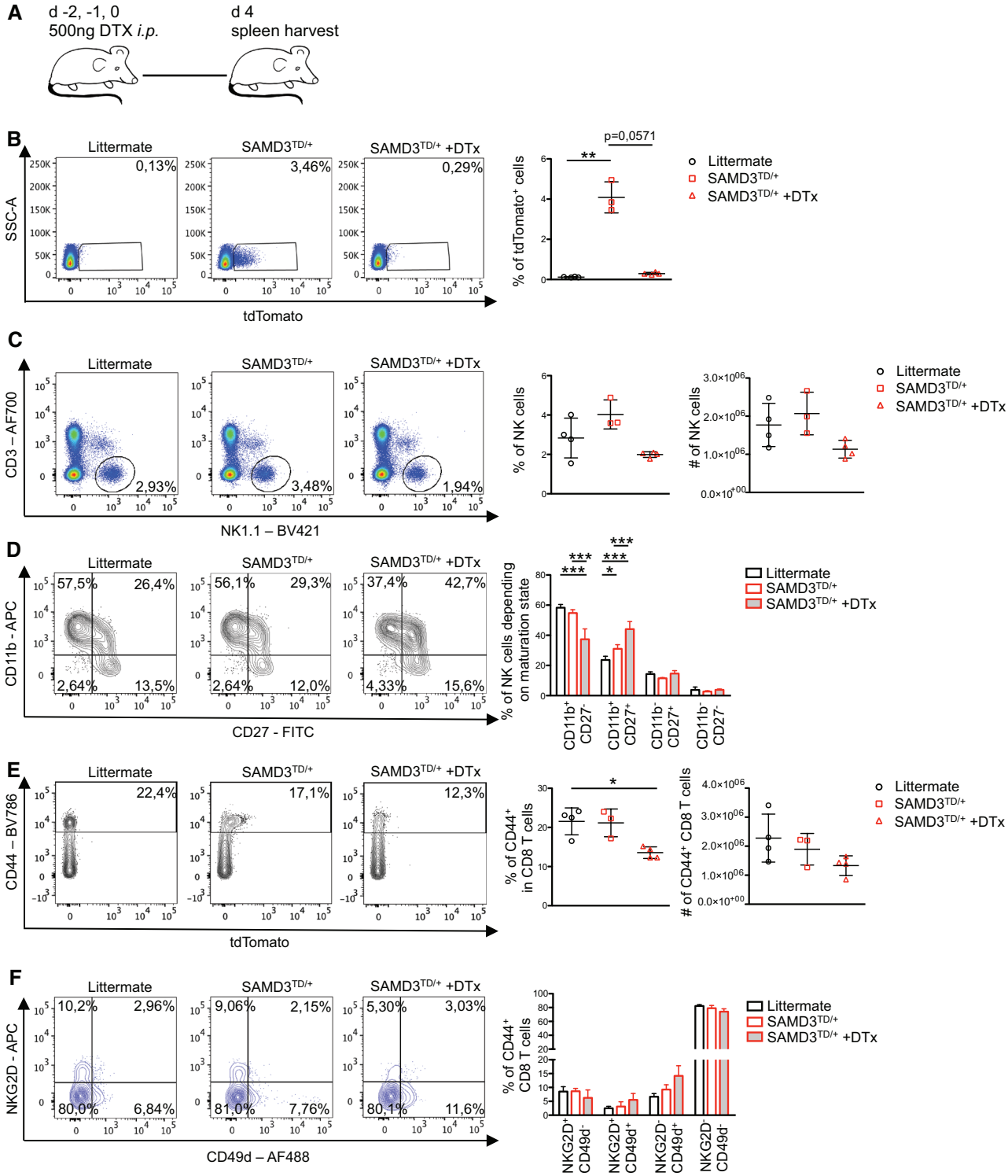

Figure 2. Samd3-expressing cell subsets are efficiently depleted by DTx treatment. (A) Experimental design. (B-F) Flow cytometry analysis of splenocytes of Samd3$^{TD/+}$ mice, Samd3$^{TD/TD}$, and littermate control mice following treatment with DTx. Representative flow cytometry plots and statistical quantification of the frequency of (B) all tdTomato+ splenocytes, (C) NK cells, (D) NK cell subsets based on CD11b and CD27 expression, (E) CD44+ CD8 T cells, and (F) CD44+ CD8 T cell subsets based on NKG2D and CD49d expression. For each panel, one representative experiment is shown. Data are representative of at least three independent experiments ($n \geq 3$ mice per experiment). Error bars indicate SD, and statistical analysis was done with one-way ANOVA (B, C, E) or two-way ANOVA (D, F) using GraphPad. *p-value < 0.05; **p-value < 0.01; ***p-value < 0.001.

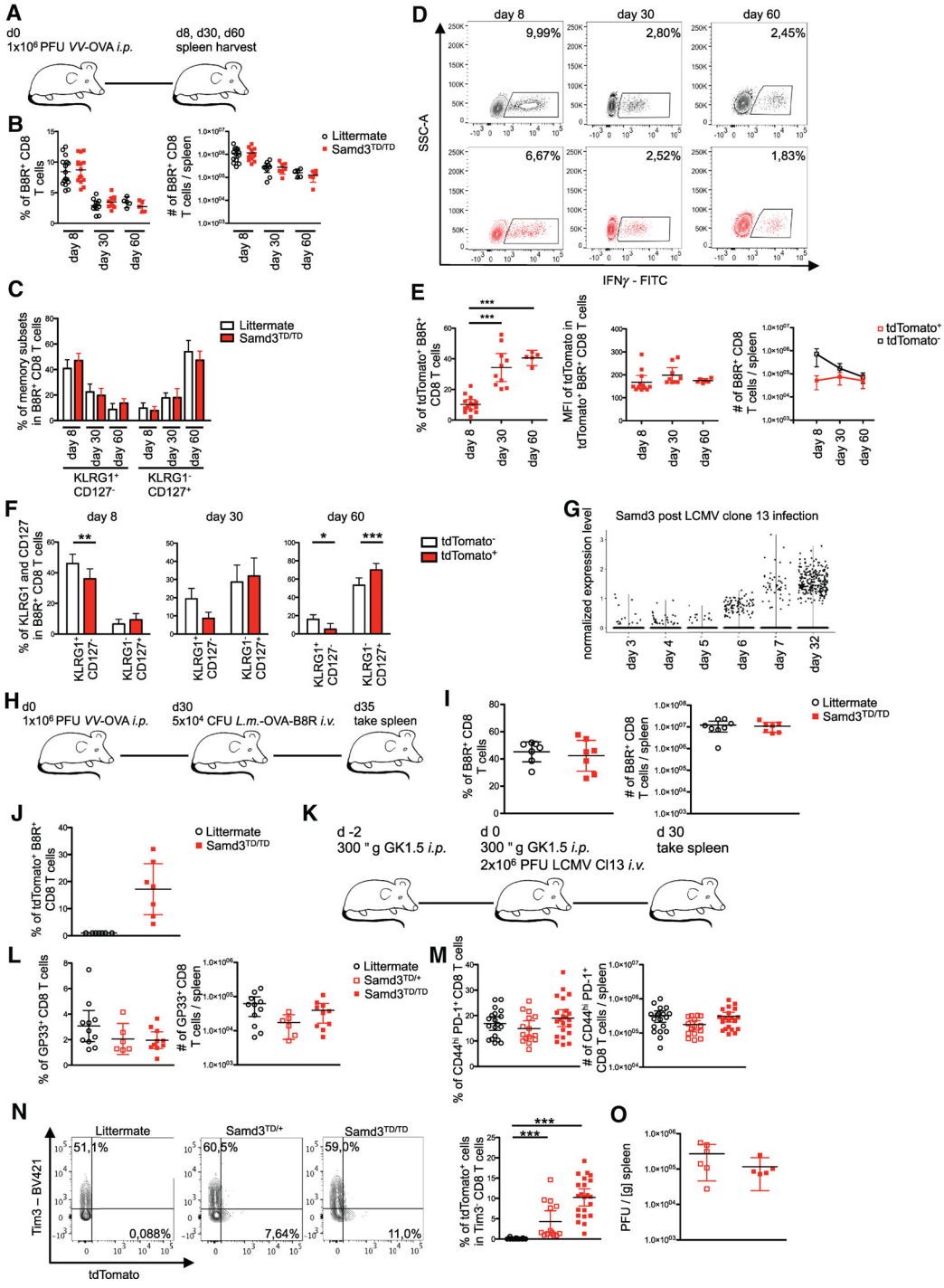

Figure 3. SAMD3 deficiency does not impact on CD8 T cell function during acute or chronic infections. (A) Experimental design for (B–F). (B–F) Flow cytometry analysis of splenocytes of Samd3$^{TD/TD}$ and littermate control mice following infection with VV-OVA (*Vaccinia* virus expressing ovalbumin). (B) Frequencies and total numbers of antigen-specific B8R$^+$ CD8 T cells (immuno-dominant epitope of *Vaccinia* virus). (C) Frequencies and statistical analysis of subsets B8R$^+$ CD8 T cells based on KLRG1 and CD127 expression. (D) Representative flow cytometry plots showing IFN-γ production in CD8 T cells following ex vivo stimulation with B8R peptide. (E) Frequencies, MFI, and total numbers of tdTomato$^+$ and tdTomato$^-$, B8R$^+$ CD8$^+$ T cells in Samd3$^{TD/TD}$ mice. (G) Violin-plot displaying normalized expression level of Samd3 on a single cell level. Cells are grouped by time point post infection with LCMV clone 13. The data were obtained from GSE131847. (H) Experimental design for I/J. (I) Frequencies and total numbers of B8R$^+$ CD8 T cells in the spleens of Samd3$^{TD/TD}$ and littermate control mice. (J) Frequency of tdTomato$^+$ B8R$^+$ CD8 T cells. (I–J) Data were measured by flow cytometry. (K) Experimental design for (L-P). (L-P) Flow cytometry analysis of splenocytes of Samd3$^{TD/+}$, Samd3$^{TD/TD}$, and littermate control mice. Frequency and total numbers of (L) tetramer-specific (GP33$^+$) and (M) PD-1$^+$ CD8$^+$ T cells after infection. (N) Representative flow cytometry plots and frequencies of tdTomato$^+$, PD-1$^+$ CD8$^+$ T cells. (O) Splenic viral titres. Data show one experiment (O, $n \geq 5$ mice) or are representative of at least two independent experiments ($n \geq 3$ mice per experiments). Error bars indicate SD, and statistical analysis was done with Student's t-test (B, I, J, O, one-way ANOVA (E, L, M, O) or two-way ANOVA (C, F)) using GraphPad Prism. *p-value ≤ 0.05; **p-value ≤ 0.01; ***p-value ≤ 0.001.

rechallenged them in the memory phase (d30) with LM-B8R that express the viral epitope $B8R_{20}$ and analyzed the spleen 5 days later (d35) (Fig. 3h). We saw a dramatic expansion of B8R-specific CD8 T cells upon rechallenge, however there was no difference in relative and absolute numbers when comparing gene-deficient *Samd3*$^{TD/TD}$ mice to littermate controls (Fig. 3i). Also, we did not observe an enrichment of tdTomato expressing cells on d5 after recall (20%) (Fig. 3j) as compared to the memory phase (d30) (Fig. 3e). CD8 T cells from *Samd3*-deficient mice showed a similar expression pattern of KLRG1, CD127, and CX_3CR1 as seen in WT littermates upon reinfection with LM-B8R (Supporting Information Fig. S6a). Also, the frequency and total numbers of IFNγ-producing antigen-specific CD8 T cells was similar between WT littermates and *Samd3*-deficient mice upon ex vivo restimulation using $B8R_{20}$ peptide (Supporting Information Fig. S6b). However, we did observe a minor reduction in the capacity to produce TNFα in this assay (Supporting Information Fig. S6c). In summary, although SAMD3 expression is highly enriched in memory CD8 T cells, SAMD3 does not seem to be required for their differentiation or their function with regard to cytokine production or proliferation in the context viral or bacterial infections.

SAMD3 is expressed in precursors of exhausted T cells but is not critical for viral control

As shown above, SAMD3 is enriched in memory CD8 T cells and may serve as a marker to identify T cells with a memory potential early after acute viral infections. Next, we aimed to investigate whether SAMD3 or SAMD3-expressing cells play an important role during chronic infections and during checkpoint immunotherapy to uncover a potential role beyond cytokine production or proliferation. To test this, we infected WT, *Samd3*$^{TD/WT}$, and *Samd3*$^{TD/TD}$ mice with LCMV clone 13 (CL13), depleted CD4 T cells prior to infection to achieve long-term viral persistence and severe exhaustion within CD8 T cells and analyzed the spleens on d30 postinfection (Fig. 3k). Both in relative and absolute numbers we detected a similar abundance of GP33-specific anti-viral CD8 T cells in WT, *Samd3*$^{TD/WT}$, and *Samd3*$^{TD/TD}$ animals (Fig. 3l). Also, globally the numbers of PD-1+ CD44hi CD8 T cells were similar between these experimental groups (Fig. 3m). PD-1 expressing cells during chronic infection can be further subdivided into exhausted T cells (T_{EX}) and precursor of exhausted CD8 T cells (T_{PEX}) that are characterized by TCF-1 expression and the absence of TIM3 on their surface. When further analyzing exhausted PD-1+ CD44hi CD8 T cells we found that tdTomato expression was restricted to T_{PEX} cells in *Samd3*$^{TD/WT}$ and *Samd3*$^{TD/TD}$ mice (Fig. 3n). This indicated that SAMD3 expression is found in a subset of Tpex—a cell population that is critical for viral control and constitutes key responders to checkpoint immunotherapy. This observation indicated that SAMD3 or *Samd3*-expressing cells may play an important role to limit viral replication during chronic infections. However, the viral titers in *Samd3*$^{TD/TD}$ and *Samd3*$^{TD/WT}$ animals were similar during the chronic phase of infection (Fig. 3o). Also, depletion *Samd3*-expressing cells during αPD-L1 therapy did not lead to significant alterations in viral titer (data not shown). In summary, SAMD3 as well as *Samd3*-expressing cells appear to be functionally redundant during chronic viral infections as tested here.

Discussion

For this study, we have developed a novel mouse model in order to address the function of the largely unstudied protein SAMD3 that we found highly expressed in memory T cells. This mouse model was developed according to a novel design concept that allowed us to address the protein function, the expression pattern, and the role of the SAMD3-expressing cells. With regard to the cellular expression pattern, we detected SAMD3 expression specifically in lymphocytes with cytotoxic capacity that are NK cells, CD8 T cells, and a fraction of invariant T cells. However, we cannot exclude that other cell types also express SAMD3 in the context of specific activation conditions that were not investigated here. In the steady state, about 65% of NK cells expressed SAMD3, yet only a small fraction of immature NK cells ($CD27^-$ /$CD11b^-$) were reporter positive. This indicates that SAMD3 expression establishes during the course of NK cell maturation and differentiation. In CD8 T cells, we started to detect SAMD3 by d6 postinfection and the fraction of SAMD3 expressing cells increased during the transition to the memory phase to about 40% of all antigen-specific CD8 T cells. Importantly, the total numbers of SAMD3-expressing cells during the contraction phase and transition to memory remained stable. Whether SAMD3-expressing cells have a better survival rate than nonexpresser or SAMD3 expression is acquired over time needs to be addressed in future experiments. In this study, we did not observe differences when comparing tdTomato-positive cells to heterozygous or homozygous Samd3-deficient reporter mice. However, a direct comparison within mice using mixed bm chimeric animals might be required to detect more subtle differences. In any case, the temporal expression pattern argues against a role of SAMD3 in the differentiation of CD8 T cells or in their effector function. In line with this conclusion, we did not detect differences in CD8 T-cell differentiation, cytokine production or viral control if *Samd3* was genetically deleted. Similarly, we did not observe differences in NK cell abundance or differentiation in the absence of SAMD3. Although our mouse model worked as anticipated we were unfortunately unable to resolve this functional role of SAMD3 in vivo. Neither during acute nor chronic viral infections SAMD3 seemed to play an important role for pathogen control. This is surprising to us since SAMD3 is a conserved protein with high homology in diverse species such as human, rat, and chimpanzee, which suggests a conserved function of this protein. Therefore, we speculate that SAMD3 is either functionally compensated or we have not applied the right experimental conditions to reveal its specific role. In this regard, it might be worthwhile to revisit this mouse model in the context of tumors or using an infection model that directly addresses the function of NK cells such as mouse CMV [21]. Additionally, future biochemical studies are required and will provide further

insights into the specific cellular functions of this protein and its subcellular localization that guide the design of future in vivo experiments.

Besides the conditional depletion of *Samd3*, our mouse model also allowed us to conditionally deplete SAMD3-expressing cells by applying DTx in vivo. For full depletion of NK cells, this model is, however, not useful since 35% of NK cells do not express SAMD3 and quickly replenish the empty niche. Similar limitations apply when depleting memory CD8 T cells and Tpex cells. Since we did not find a specific role of SAMD3 positive versus negative memory CD8 T cells, we conclude that DTx-mediated depletion will primarily impact on the quantity of the remaining memory population rather than on their quality.

In summary, we have developed and validated a new mouse model to study the roles of SAMD3 by combining conditional genetic deletion, a reporter function, and conditional depletion of SAMD3-expressing cells. Although we were not able to define a functional role for SAMD3, we have characterized the cellular and temporal expression pattern of this poorly studied protein and investigated its function in acute and chronic viral infections. We hope that the novel design concept of our mouse model will be applied to other loci to study novel genes and their functional significance.

Materials and methods

Animals

B6.B6-Samd3$^{myrtdT\text{-}DTR2WK}$/J (Samd3) mouse line was generated in co-operation with Ozgene and kept in an in-house facility. Mice were bred against a ubiquitous Cre recombinase mouse line (Ub-Cre/Oz-Cre) in the Ozgene facility and were then used in this study. All mice were kept in specific pathogen-free conditions at an Association for Assessment and Accreditation of Laboratoy Animal Care-accredited animal facility. All procedures were approved by the North Rhine-Westphalia State Environment Agency (LUA NRW) and the Bavarian State Environment Agency (ROB).

Genotyping PCRs and southern blots

Genotyping PCRs were established and ran on tissue samples generated during necessary ear-marking process. DNA was isolated by digesting tissue sample in 50 mM NaOH mixed with 10 mM EDTA (final concentration 0.2 mM) for 1 h at 95°C. Digestion was stopped by adding 1 M Tris-HCl (pH 8; final concentration 0.1 M). The PCR reaction was run using Sigma Taq Polymerase (Sigma-Aldrich; Order-no. 9012-90-2) following manufacturer's protocol. Primer sequences of the used primers for the PCR reactions were as follows: primer_01F 5′-TGGAAACGTGGTCAGTTGATCAG-3′; primer_02R 5′-CCAAGAGTTTGCAATCATCTGG-3′; primer_03F 5′-CTACCCGTGATATTGCTGAAGAGC-3′; primer_04R 5′-GAAGAGAAAGTGAAGTTGGGCATG-3′. Southern blots were performed by Ozgene.

Flow cytometry analysis (surface and intracellular staining)

In this project, we adhered to the general guidelines for flow cytometry [22]. Single cell suspension obtained from spleens were used for flow cytometry analysis using BD Canto II, BD Fortessa or Attune (Thermo Fisher Scientific). Cells were surface stained with near-IR life/dead stain (Thermo Fisher Scientific), anti-CD8 (BioLegend; clone: 53–6.7), anti-CD44 (BioLegend, BD; clone: IM7), anti-PD-1 (BioLegend; clone: 29F.1A12), anti-KLRG1 (eBioscience; clone: 2F1), anti-CD127 (BioLegend; clone: SB/199), anti-CX_3CR1 (BioLegend; clone: SAO11F11), anti-Tim3 (R&D, BioLegend; clones: FAB1529G, RMT3-23), anti-CD3 (BioLegend; clone: 17A2), anti-NK1.1 (BioLegend; clone: PK136), anti-CD4 (BD, BioLegend; clones: GK1.5, RM4-5), anti-γδTCR (eBioscience; clone: eBioGL3), anti-Vβ6/Vβ8 TCR (BioLegend; clone: H57.597), anti-CD11b (eBioscience; clone: M1/70), anti-CD27 (eBioscience; clone: LG.7F9), anti-NKG2D (eBioscience; clone: CX5), and anti-CD49d (BioLegend; clone: R1-2). Antigen-specific CD8 T cells were identified by using tetramers binding to the immunodominant TCR in the infection model. Gp33 tetramer (H2-Db, LCMV GP 33–41, NIH Tetramer Core Facility) and B8R dextramer (H2-Kb *Vaccinia* virus B8R 20–27, Immudex) were used. For intracellular staining, single cell suspensions were activated before surface staining by antigen-specific peptide in combination with Brefeldin A (eBioscience) for 4 h at 37°C. Next, surface staining was performed followed by fixation and permeabilization using BD FixPerm solution. Single cell suspension was stained in permeabilization wash buffer (1×) (BD) using anti-IFNγ (BioLengend; clone: XMG1.2), anti-TNFα (BioLegend; clone: MD6-XT22), and anti-IL2 (eBioscience; clone: JES6-5K4).

Treatment of mice

For depletion of cell populations by diphtheria toxin (DTx) (Merck Millipore), mice were injected 0.5 mg DTx intraperitoneal (i.p.) on three consecutive days. For infection with VV-OVA [23], mice were infected i.p. with 1×10^6 PFU. For infection with LM-B8R, mice were infected intravenously (i.v.) with 5×10^4 CFU. For infection with chronic LCMV clone 13, 2×10^6 IU were applied i.v. after treating the mice 2 days prior and on the day of infection with 300 μg anti-CD4 (GK1.5, BioXcell) i.p.

Generation/production of viruses and bacteria

Attenuated strain LM-B8R (expressing the B8R epitope from vaccinia virus) [24] was provided by Dr. Ross Kedl (National

Jewish Medical Research Center, University of Colorado, Denver, CO). LM-B8R was grown in BHI medium. After overnight culture, a log culture was set up and at an $OD_{600} = 0.1 – 0.3$, the bacteria were harvested and diluted in PBS. For the propagation of the viruses, appropriate cell lines (L929 cells for LCMV and DF-1 cells for *Vaccinia* virus) were cultivated and infected with a MOI = 0.01 from virus stocks. Supernatants or cell lysates containing the viral particles were collected after 24 h, 48 h, and 72 h. For LCMV clone 13, the supernatant was sterile filtered while for VV-OVA cell lysates were purified using two consecutive sucrose cushions. Viral titration for LCMV clone 13 was done as described below. For *Vaccinia* virus, a serial dilution on DF-1 cells was performed and the formation of viral plaques was monitored as a read-out.

Viral titration LCMV clone 13

Titration of the LCMV clone 13 was performed on MC57G cells. Serial dilutions in the range of 2×10^{-2} to 2×10^{-6} were performed and added to the cells. Note that 48 h later medium was changed, and incubation continued for another 24 h. Then medium was aspirated, cells were washed in PBS and fixed with Cytofix/Cytoperm (BD). After blocking free binding sites with fetal cow serum, cells were incubated with a 1:10 dilution of hybridomal supernatant from VL-4 cell line for 1 h. Counterstaining of the hybridomal antibodies binding to the nucleoprotein of the LCMV with anti-rat-IgG-AF488 (Invitrogen) was analyzed under a fluorescent microscope.

RNA-sequencing data processing and analysis

For the presented bulk and scRNA-sequencing results, published datasets were analyzed running a customized R script with DESeq2 [25] for bulk-sequencing data or Seurat v.3.1 [26] for single cell sequencing. Raw counts of the published data were used (GEO Accession: GSE109125 [27]; GSE131847 [19, 20]).

Statistical analysis

Apart of the genomic data, all biological data were analyzed using Prism 8 software (GraphPad) by two-tailed paired Student's *t*-test, two-tailed unpaired Student's *t*-test, or one- and two-way ANOVA test.

Acknowledgements: We would like to thank the Core Unit for FACS and the Core Unit SysMed of the IZKF Würzburg for supporting this study. The GP33 tetramer was obtained through the NIH Tetramer Core Facility. We thank M. Väth and M. Ugur for critically reading the manuscript. This work was funded by grants through the NRW-Rückkehrerprogramm of the German state of Northrhine-Westfalia to W.K. W.K. is further supported by the University of Würzburg and the Max Planck Society (Max Planck Research Groups).

Conflict of Interest: The authors declare to have no commercial or financial conflict of interest.

Ethics Statement: The animal experiments used in this study were reviewed and approved by the local authorities.

Author Contributions: A.E.P., K.K., and W.K. participated in research design. A.E.P., K.K., A.G., and W.K. conducted experiments. A.E.P., K.K., A.G., and W.K. performed data analysis. A.E.P. and W.K wrote the manuscript.

Data Availability Statement: The raw data supporting the conclusion of this article will be made available by the authors, without undue reservation.

Peer review: The peer review history for this article is available at https://publons.com/publon/10.1002/eji.202149469

References

1 **Kaech, S. M.** and **Cui, W.**, Transcriptional control of effector and memory CD8+ T cell differentiation. *Nat. Rev. Immunol.* 2012. **12**(11): 749–761.

2 **Salerno, F.**, **Turner, M.** and **Wolkers, M. C.**, Dynamic post-transcriptional events governing CD8(+) T cell homeostasis and effector function. *Trends Immunol.* 2020. **41**(3): 240–254.

3 **Kastenmuller, W.**, **Brandes, M.**, **Wang, Z.**, **Herz, J.**, **Egen, J. G.** and **Germain, R. N.**, Peripheral prepositioning and local CXCL9 chemokine-mediated guidance orchestrate rapid memory CD8+ T cell responses in the lymph node. *Immunity* 2013. **38**(3): 502–513.

4 **Qi, H.**, **Kastenmuller, W.** and **Germain, R. N.**, Spatiotemporal basis of innate and adaptive immunity in secondary lymphoid tissue. *Annu. Rev. Cell Dev. Biol.* 2014. **30**: 141–167.

5 **Gebhardt, T.**, **Wakim, L. M.**, **Eidsmo, L.**, **Reading, P. C.**, **Heath, W. R.** and **Carbone, F. R.**, Memory T cells in nonlymphoid tissue that provide enhanced local immunity during infection with herpes simplex virus. *Nat. Immunol.* 2009. **10**(5): 524–530.

6 **Samji, T.** and **Khanna, K. M.**, Understanding memory CD8(+) T cells. *Immunol. Lett.* 2017. **185**: 32–39.

7 **Chen, Y.**, **Zander, R.**, **Khatun, A.**, **Schauder, D. M.** and **Cui, W.**, Transcriptional and epigenetic regulation of effector and memory CD8 T cell differentiation. *Front. Immunol.* 2018. **9**: 2826.

8 **Cui, G.**, **Staron, M. M.**, **Gray, S. M.**, **Ho, P. C.**, **Amezquita, R. A.**, **Wu, J.** and **Kaech, S. M.**, IL-7-induced glycerol transport and TAG synthesis promotes memory CD8+ T cell longevity. *Cell* 2015. **161**(4): 750–761.

9 **Roberts, A. B.**, **Russo, A.**, **Felici, A.** and **Flanders, K. C.**, Smad3: a key player in pathogenetic mechanisms dependent on TGF-beta. *Ann. N. Y. Acad. Sci.* 2003. **995**: 1–10.

10 **Kim, C. A.** and **Bowie, J. U.**, SAM domains: uniform structure, diversity of function. *Trends Biochem. Sci.* 2003. **28**(12): 625–628.

11 **Li, H.**, **Fung, K. L.**, **Jin, D. Y.**, **Chung, S. S.**, **Ching, Y. P.**, **Ng, I. O.**, **Sze, K. H.** et al., Solution structures, dynamics, and lipid-binding of the sterile

alpha-motif domain of the deleted in liver cancer 2. *Proteins* 2007. **67**(4): 1154–1166.

12 **Spits, H., Artis, D., Colonna, M., Diefenbach, A., Di Santo, J. P., Eberl, G., Koyasu, S.** et al., Innate lymphoid cells—a proposal for uniform nomenclature. *Nat. Rev. Immunol.* 2013. **13**(2): 145–149.

13 **Abel, A. M., Yang, C., Thakar, M. S.** and **Malarkannan, S.**, Natural killer cells: development, maturation, and clinical utilization. *Front. Immunol.* 2018. **9**: 1869.

14 **Chiossone, L., Chaix, J., Fuseri, N., Roth, C., Vivier, E.** and **Walzer, T.**, Maturation of mouse NK cells is a 4-stage developmental program. *Blood*. 2009. **113**(22): 5488–5496.

15 **Grau, M., Valsesia, S., Mafille, J., Djebali, S., Tomkowiak, M., Mathieu, A. L., Laubreton, D.** et al., Antigen-induced but not innate memory CD8 T cells express NKG2D and are recruited to the lung parenchyma upon viral infection. *J. Immunol.* 2018. **200**(10): 3635–3646.

16 **White, J. T., Cross, E. W.** and **Kedl, R. M.**, Antigen-inexperienced memory CD8(+) T cells: where they come from and why we need them. *Nat. Rev. Immunol.* 2017. **17**(6): 391–400.

17 **Bottcher, J. P., Beyer, M., Meissner, F., Abdullah, Z., Sander, J., Hochst, B., Eickhoff, S.** et al., Functional classification of memory CD8(+) T cells by CX3CR1 expression. *Nat. Commun.* 2015. **6**: 8306.

18 **Gerlach, C., Moseman, E. A., Loughhead, S. M., Alvarez, D., Zwijnenburg, A. J., Waanders, L., Garg, R.** et al., The chemokine receptor CX3CR1 defines three antigen-experienced CD8 T cell subsets with distinct roles in immune surveillance and homeostasis. *Immunity* 2016. **45**(6): 1270–1284.

19 **Kurd, N. S., He, Z., Louis, T. L., Milner, J. J., Omilusik, K. D., Jin, W., Tsai, M. S.** et al., Early precursors and molecular determinants of tissue-resident memory CD8(+) T lymphocytes revealed by single-cell RNA sequencing. *Sci Immunol*. 2020. **5**(47): eaaz6894.

20 **Milner, J. J., Toma, C., He, Z., Kurd, N. S., Nguyen, Q. P., McDonald, B., Quezada, L.** et al., Heterogenous populations of tissue-resident CD8(+) T cells are generated in response to infection and malignancy. *Immunity* 2020. **52**(5): 808–824. e7.

21 **Sun, J. C., Beilke, J. N.** and **Lanier, L. L.**, Adaptive immune features of natural killer cells. *Nature* 2009. **457**(7229): 557–461.

22 **Cossarizza, A., Chang, H. D., Radbruch, A., Acs, A., Adam, D., Adam-Klages, S., Agace, W. W.** et al., Guidelines for the use of flow cytometry and cell sorting in immunological studies (second edition). *Eur. J. Immunol.* 2019. **49**(10): 1457–1973.

23 **Eickhoff, S., Brewitz, A., Gerner, M. Y., Klauschen, F., Komander, K., Hemmi, H., Garbi, N.** et al., Robust anti-viral immunity requires multiple distinct T cell-dendritic cell interactions. *Cell* 2015. **162**(6): 1322–1337.

24 **Olson, J. A., McDonald-Hyman, C., Jameson, S. C.** and **Hamilton, S. E.**, Effector-like CD8(+) T cells in the memory population mediate potent protective immunity. *Immunity* 2013. **38**(6): 1250–1260.

25 **Love, M. I., Huber, W.** and **Anders, S.**, Moderated estimation of fold change and dispersion for RNA-seq data with DESeq2. *Genome Biol.* 2014. **15**(12): 550.

26 **Stuart, T., Butler, A., Hoffman, P., Hafemeister, C., Papalexi, E., Mauck W. M., 3rd, Hao, Y.** et al., Comprehensive integration of single-cell data. *Cell*. 2019. **177**(7): 1888–1902. e21.

27 **Yoshida, H., Lareau, C. A., Ramirez, R. N., Rose, S. A., Maier, B., Wroblewska, A., Desland, F.** et al., The cis-regulatory atlas of the mouse immune system. *Cell*. 2019. **176**(4): 897–912. e20.

Full correspondence: Dr. Annika E. Peters and Prof. Wolfgang Kastenmüller, Würzburg Institute of Systems Immunology, Max Planck Research Group at the Julius-Maximilians-Universität Würzburg, Wurzburg, Germany
e-mail: Annika.Peters@med.uni-muenchen.de; wolfgang.kastenmueller@uni-wuerzburg.de

Received: 22/6/2021
Revised: 30/8/2021
Accepted: 6/10/2021
Accepted article online: 9/10/2021